coatings

Supplementary Materials: Simultaneous Precipitation and Electrodeposition of Hydroxyapatite Coatings at Different Temperatures on Various Metal Substrates

Bogdan-Ovidiu Taranu, Paula Ianasi, Stefania Florina Rus and Alexandra Ioana Bucur*

National Institute for Research and Development in Electrochemistry and Condensed Matter, Dr. A. Paunescu Podeanu Street, No. 144, 300569 Timisoara, Romania; b.taranu84@gmail.com (B.-O.T.); paulasvera@gmail.com (P.I.); rusflorinastefania@gmail.com (S.F.R.)
* Correspondence: alexandra.i.bucur@gmail.com

Citation: Taranu, B.-O.; Ianasi, P.; Rus, S.F.; Bucur, A.I. Simultaneous Precipitation and Electrodeposition of Hydroxyapatite Coatings at Different Temperatures on Various Metal Substrates. *Coatings* **2022**, *12*, 288. https://doi.org/10.3390/coatings12020288

Academic Editor: Lech Pawlowski

Received: 20 December 2021
Accepted: 18 February 2022
Published: 21 February 2022

In brief literature data regarding the electrodeposition of HA on various metal substrates

Qiu et al. [1] reported that HA and HA/ZnO_2 composite coatings were electrodeposited on NiTi alloy and significantly improved the corrosion resistance of the substrate, which is a matter of concern in the absence of the electrodeposited coating. Nickel supports were also used [2] as indirect substrates for the electrodeposition of HA coatings using the standard method. Basically, the substrates were made from Ti covered with a nanometric Ni layer, on top of which vertically aligned multiwall carbon nanotubes were synthesized.

Liu et al. [3] successfully coated HA on various metal substrates (Ti, stainless steel 316L, Cu and Al) by a seeded hydrothermal deposition method, according to which the hydrothermal crystallization stage is preceded by the short electrochemical deposition of a HA seed layer.

No articles have been found that report the electrodeposition of HA on C55 stainless steel substrate. The most similar studies published in the literature for the electrodeposition of HA using the standard method are those on stainless steels with other compositions than C55. It should be noted that while the standard method refers to the electrodeposition of HA from an electrolyte solution containing both the Ca and P precursors, it does not preclude the presence of other substances in this solution that serve different roles, such as H_2O_2 and $NaNO_3$ [4]. Due to its application in dental and orthopedic implants, the 316L stainless steel is the metal support of choice for most studies conducted on HA coatings electrodeposited onto stainless steel substrates [4–7]. However, stainless steels with different compositions have also been used for the same purpose. For example, the 316 stainless steel, having a similar composition to that of 316L, has been employed as substrate in the pulsed electrodeposition of biocompatible hydroxyapatite coatings that increase the tissue growth rate over the surface of the implants [8]. HA was also electrodeposited in continuous, pulsed and pulsed reverse mode on the same type of metallic substrate by Chakraborty et al. [9], as well as chronopotentiometrically on a specific reference 316 stainless steel by Chennah et al. [10]. Other types of metal substrates that were covered with electrodeposited HA coatings are 304 stainless steel [11] and duplex stainless steel S2205 [12].

As far as the use of copper supports for HA coatings electrodeposition goes, the previously mentioned study by Liu et al. [3] is the most similar to the one described in the present paper, in which the standard method is employed to electrodeposit HA on copper substrate. Other studies from the literature that involve the use of copper and HA concern the coating of Ti substrates with electrosynthesized Cu-HA composites [13] or electrodeposited co-substituted HA, with Cu being one of the substitution cations [14,15].

Examples of AFM investigations of HA coatings on titanium and stainless steel

One example is the AFM analysis performed on HA coatings electrodeposited on Ti substrate reported by Eliaz and Eliyahu [16]. The researchers coated HA layers on Ti and Ti alloy substrates using the standard electrochemical deposition method at a constant temperature within the 60–90°C range. The study of the nucleation and growth of HA was accomplished *via* electrochemical AFM imaging, and the results show that HA is electrodeposited from precipitation in solution following an initial stage of instantaneous nucleation and a subsequent step of progressive nucleation. As for the applied electrodeposition potential, a negative value higher than -1.26 V vs. SCE is required to enhance HA growth, which includes the value used in the current study (-1.545 V vs. SCE). The AFM results obtained by Durairaj *et al.* [17] on HA coatings electrodeposited over etched Ti substrates, using the standard method and an applied potential of 5V at 80°C for 1h, show an average surface roughness of ~ 6.67 nm and HA grain sizes between 17 and 36 nm. Huang *et al.* [18] used AFM analysis to characterize HA coatings on pretreated Ti substrates. The deposition procedure was divided into three stages: an electrodeposition stage in electrolyte solution containing both HA precursors, a hydrothermal treatment stage and a sintering stage. AFM micrographs recorded on the HA coatings revealed the porous nature of the deposition - with a mean pore size of 236.5 μm - and the absence of any cracks.

AFM investigations of HA electrodeposited on copper and nickel supports do not seem to have been reported in the scientific literature, but there are such studies performed on HA covered stainless steel supports [19,20]. For example, Thom *et al.* [20] synthesized hydroxyapatite and hydroxyapatite/carbon nanotubes as coatings on the surface of 316L stainless steel substrates, by the standard electrodeposition technique. AFM images obtained on the samples coated with HA only show an average roughness about 10 times higher than that of the uncoated metal support (241±20 nm *vs.* 21±2 nm).

The first comparative study

Figure S1 shows selected images recorded during the thickness investigations.

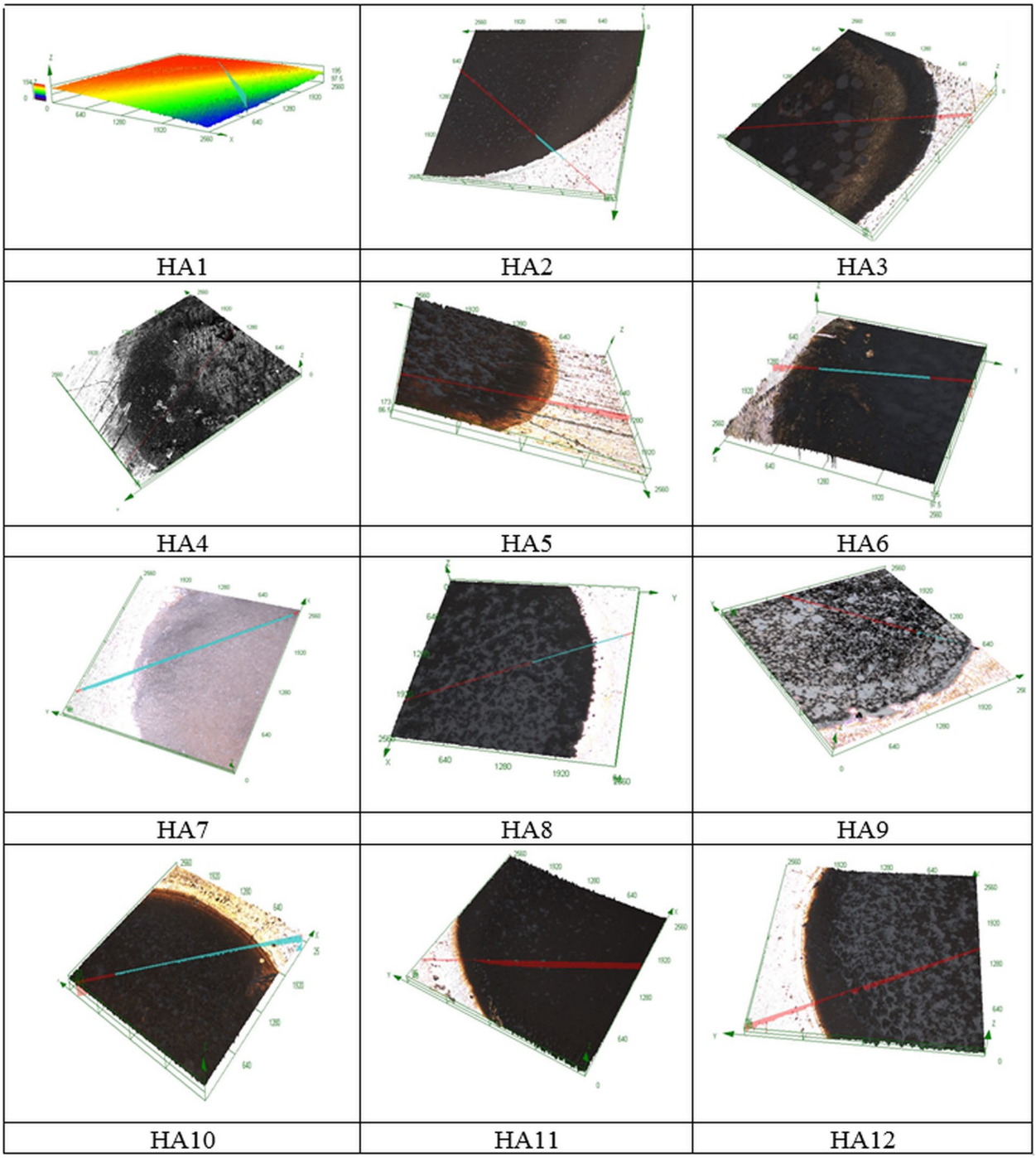

Figure S1. Selected micrographs recorded during the laser microscopy analysis of the HA1-HA12 samples.

Table S1 shows the mean values obtained from AFM surface analysis of the HA1-HA12 specimens.

Table S1. Mean values obtained from AFM surface analysis of the HA1-HA12 specimens.

Specimen code	Area [μm²]	Sa [nm]	Sq [nm]	Sp [nm]	Sv [nm]	Sy [nm]	Sku [xx]	Ssk [xx]
HA1	5 × 5	35.332 ±6.067	45.115 ±7.344	185.335 ±18.793	-169.27 ±43.139	354.605 ±61.932	3.687 ±0.328	0.243 ±0.097
HA2	5 × 5	125.25 ±10.5	161.5 ±18	796.6 ±84.5	-610 ±58.25	1406.6 ±142.75	6.528 ±0.353	0.215 ±0.032
HA3	5 × 5	52.526 ±3.104	66.8923 ±3.396	200.095 ±25.375	-211.262 ±25.05	411.357 ±50.425	4.1047 ±1.054	0.1148 ±0.038
HA4	5 × 5	63.903 ±3.254	78.922 ±4.24	235.58 ±15.931	-286.618 ±23.117	522.198 ±39.048	2.2876 ±0.343	-0.2046 ±0.04
HA5	5 × 5	123 ±22.5	153 ±27	435 ±79	-537 ±101	972 ±0.180	3.755 ±0.282	-0.27 ±0.03
HA6	5 × 5	57.2531 ±16.647	72.569 ±20.673	259.766 ±51.317	-236.48 ±60.08	496.246 ±111.397	3.316 ±0.188	0.353 ±0.073
HA7	5 × 5	51.314 ±17.96	64.778 ±22.794	199.996 ±46.13	-235.318 ±59.32	435.314 ±105.45	3.89 ±1.335	-0.0066 ±0.02
HA8	5 × 5	85.994 ±24.775	107.411 ±30.959	280.988 ±70.185	-394.871 ±88.526	675.859 ±158.711	3.843 ±1.445	-0.375 ±0.116
HA9	5 × 5	33 ±8	42.1 ±10	133 ±16	-145 ±31	278 ±47	4.402 ±1.69	0.205 ±0.02
HA10	5 × 5	86.837 ±31.574	106.086 ±36.841	322.496 ±96.096	-322.492 ±90.485	644.988 ±186.581	3.43 ±1.0615	0.0006 ±0.037
HA11	5 × 5	95.278 ±36.94	118.029 ±43.858	304.221 ±91.108	-369.378 ±81.475	673.6 ±172.583	3.698 ±1.046	0.104 ±0.03
HA12	5 × 5	83 ±11.5	104.7 ±12.5	288 ±30	-345 ±35	633 ±65	4.263 ±1.17	-0.23 ±0.03

The second comparative study

Figure S2 presents examples of images obtained during the thickness analysis.

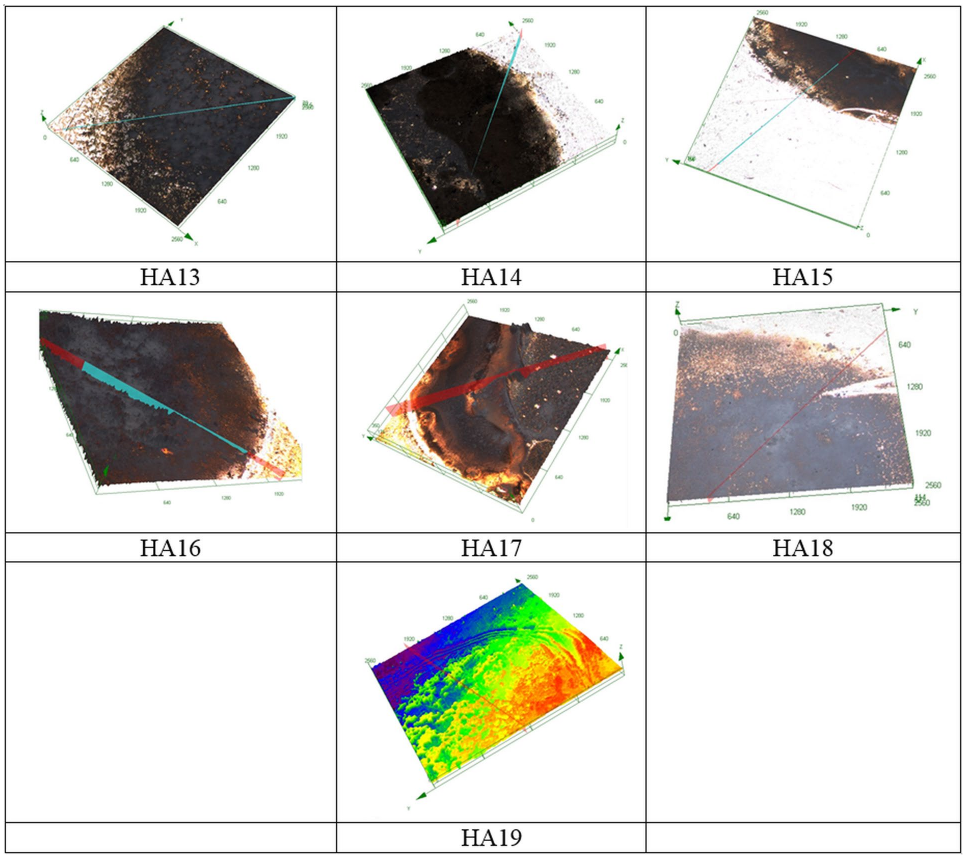

Figure S2. Selected micrographs recorded during the laser microscopy analysis of the HA13–HA19 samples.

Table S2 shows the mean values obtained from AFM surface analysis of the HA3 and HA13-HA19 specimens.

Table S2. Mean values obtained from AFM surface analysis of the HA3 and HA13-HA19 specimens.

Specimen code	Area [μm²]	Sa [nm]	Sq [nm]	Sp [nm]	Sv [nm]	Sy [nm]	Sku	Ssk
HA13	5 × 5	52.808 ±10.851	67.213 ±13.278	262.204 ±36.038	-223.781 ±24.552	485.781 ±60.59	4.4188 ±1.52	0.3705 ±0.093
HA3	5 × 5	52.526 ±3.104	66.8923 ±3.396	200.095 ±25.375	-211.262 ±25.05	411.357 ±50.425	4.1047 ±1.44	0.1148 ±0.038
HA14	5 × 5	98.95 ±7.05	127.58 ±11.7	437.18 ±81.43	-515.78 ±56.27	953 ±137.7	3.79 ±0.417	-0.36 ±0.048
HA15	5 × 5	47.345 ±15.295	59.27 ±17.612	233.938 ±47.288	-185.932 ±55.956	419.87 ±103.244	4.147 ±1.031	0.458 ±0.084
HA16	5 × 5	132.5 ±22.81	158.75 ±23.82	392.167 ±31.63	-423.5 ±42.37	815.667 ±74	2.42 ±0.338	-0.134 ±0.016
HA17	5 × 5	54.579 ±17.083	68.025 ±21.371	217.644 ±60.833	-227.993 ±63.943	445.637 ±124.776	3.7623 ±1.452	0.1966 ±0.055
HA18	5 × 5	74.233 ±6.23	92.35 ±7.41	290.5 ±22.91	-285 ±14.97	575.5 ±37.88	2.843 ±0.812	-0.09 ±0.022
HA19	5 × 5	55.4873 ±12.116	71.155 ±14.982	319.386 ±58.726	-227.274 ±48.58	546.66 ±107.306	4.649 ±1.247	0.404 ±0.1

References

1. Qiu, D.; Wang, A.; Yin, Y. Characterization and corrosion behavior of hydroxyapatite/zirconia composite coating on NiTi fabricated by electrochemical deposition. *Appl. Surf. Sci.* **2010**, *257*, 1774–1778.
2. Lobo, A.; Marciano, F.R.; Matsushima, J.T.; Ramos, S.C.; Corat, E.J. Influence of temperature and time for direct hydroxyapatite electrodeposition on superhydrophilic vertically aligned carbon nanotube films. *J. Nanomed. Nanotechnol.* **2011**, *6*, 6–11.
3. Liu, D.; Savino, K.; Yates, M.Z. Coating of hydroxyapatite films on metal substrates by seeded hydrothermal deposition. *Surf. Coat. Technol.* **2011**, *205*, 3975–3986
4. Thanh, D.T.M.; Nam, P.T.; Phuong, N.T.; Que, L.X.; Van Anh, N.; Hoang, T.; Lam, T.D. Controlling the electrodeposition, morphology and structure of hydroxyapatite coating on 316L stainless steel. *Mater. Sci. Eng. C* **2013**, *33*, 2037–2045.
5. Stefan, L.G.; Abrudeanu, M.; Iosub, I.; Plaiasu, A.G.; Dinu, A.; Mihalache, M. Electrodeposition of hydroxyapatite coatings on stainless steel 316 L. *Sci. Bull. Automot. Ser.* **2009**, *A*, 129–134
6. Gopi, D.; Indira, J.; Kavitha, L. A comparative study on the direct and pulsed current electrodeposition of hydroxyapatite coatings on surgical grade stainless steel. *Surf. Coat. Technol.* **2012**, *206*, 2859–2869.
7. Büyüksağiş, A.; Bulut, E.; Kayalı, Y. Corrosion behaviors of hydroxyapatite coated by electrodeposition method of Ti6Al4V, Ti and AISI 316L SS substrates. *Prot. Met. Phys. Chem. Surf.* **2013**, *49*, 776–787.
8. Chakraborty, R.; Sengupta, S.; Saha, P.; Das, K.; Das, S. Synthesis of calcium hydrogen phosphate and hydroxyapatite coating on SS316 substrate through pulsed electrodeposition. *Mater. Sci. Eng. C* **2016**, *69*, 875–883.
9. Chakraborty, R.; Saha, P. A comparative study on surface morphology and electrochemical behaviour of hydroxyapatite-calcium hydrogen phosphate composite coating synthesized in-situ through electro chemical process under various deposition conditions. *Surf. Interfaces* **2018**, *12*, 160–167.
10. Chennah, A.; Naciri, Y.; Ahsaine, H.A.; Taoufyq, A.; Bakiz, B.; Bazzi, L.; Guinneton, F.; Gavarri, J.R.; Benlhachemi, A. Electrocatalytic properties of hydroxyapatite thin films electrodeposited on stainless steel substrates. *Mediterr. J. Chem.* **2018**, *6*, 255–266.
11. Saremi, M.; Sabet, F.H. Nano hydroxyapatite coating on stainless steel 304 by electrochemical method. *Int. J. Mod. Phys. B* **2008**, *22*, 3092–3098.
12. Adhitya, K. Electrophoretic deposition of calcium phosphate ceramics over duplex stainless steel (S2205) and its characterization. *Int. Res. J. Eng. Technol.* **2020**, *7*, 1905–1909.
13. Ghosh, R.; Swart, O.; Westgate, S.; Miller, B.L.; Yates, M.Z. Antibacterial copper-hydroxyapatite composite coatings via electrochemical synthesis. *Langmuir* **2019**, *35*, 5957–5966.
14. Huang, Y.; Zhang, X.; Mao, H.; Li, T.; Zhao, R.; Yan, Y.; Pang, X. Osteoblastic cell responses and antibacterial efficacy of Cu/Zn co-substituted hydroxyapatite coatings on pure titanium using electrodeposition method. *RSC Adv.* **2015**, *5*, 17076–17086.

15. Huang, Y.; Hao, M.; Nian, X.; Qiao, H.; Zhang, X.; Zhang, X.; Song, G.; Guo, J.; Pang, X.; Zhang, H. Strontium and copper co-substituted hydroxyapatite-based coatings with improved antibacterial activity and cytocompatibility fabricated by electrodeposition. *Ceram. Int.* **2016**, *42*, 11876–11888.
16. Eliaz, N.; Eliyahu, M. Electrochemical processes of nucleation and growth of hydroxyapatite on titanium supported by real-time electrochemical atomic force microscopy. *J. Biomed. Mater. Res. Part A* **2006**, *80*, 621–634.
17. Durairaj, R.B.; Ramachandran, S. Corrosion characteristics of hydroxyapatite coated titanium substrate for biomedical applications. *Int. J. Chem. Sci.* **2016**, *14*, 2157–2163.
18. Huang, S.; Zhou, K.; Huang, B.; Li, Z.; Zhu, S.; Wang, G. Preparation of an electrodeposited hydroxyapatite coating on titanium substrate suitable for in-vivo applications. *J. Mater. Sci. Mater. Med.* **2008**, *19*, 437–442.
19. Gopi, D.; Collins Arun Prakash, V.; Kavitha, L.; Kannan, S.; Bhalaji, P.R.; Shinyjoy, E.; Ferreira, J.M.F. A facile electrodeposition of hydroxyapatite onto borate passivated surgical grade stainless steel. *Corros. Sci.* **2011**, *53*, 2328–2334.
20. Thom, N.T.; Nam, P.T.; Phuong, N.T.; Thi, D.; Thanh, M. Investigation of the condition to synthesize HAp/CNTs coatings on 316LSS. *Vietnam J. Sci. Technol.* **2018**, *56*, 50–62.